EuO. I. Resistivity and Hall Effect in Fields up to 150 kOe

Y. Shapira and S. Foner
Francis Bitter National Magnet Laboratory, Massachusetts Institute of Technology, Cambridge, Massachusetts 02139*

T. B. Reed†
Lincoln Laboratory, Massachusetts Institute of Technology, Lexington, Massachusetts 02173
(Received 1 March 1973)

The resistivity ρ and the Hall effect are studied in seven n-type EuO single-crystal samples at temperatures $4.2 \leq T \leq 300$ K and external magnetic fields $0 \leq H_{ext} \leq 150$ kOe. Attention is focused on three phenomena: (i) the anomalous Hall effect (or lack thereof), (ii) the resistivity peak near the Curie temperature $T_C \simeq 69$ K, and (iii) the insulator-metal transition (IMT). The Hall data at $T \ll T_C$ indicate that the anomalous Hall term in EuO is small compared to the normal term and that the effective magnetic field which governs the Hall effect is equal to the magnetic induction $B = H_{int} + 4\pi M$. On this basis it is assumed that the anomalous Hall effect is negligible at all temperatures. Measurements of $\rho(H_{ext}, T)$ vs T, show that as H_{ext} increases the resistivity peak decreases, becomes broader, and shifts to higher temperatures. The Hall data indicate that the resistivity peak is due to the combined effect of dips in the Hall mobility μ and in the carrier concentration n. Measurements of T_C by several methods show that T_C is several degrees lower than the temperature T_{max} at which the zero-field resistivity is maximum. A new method for obtaining T_C from magnetoresistance measurements is discussed. Near room temperature the resistivity of some samples decreases exponentially with increasing T, with an activation energy of ~ 0.3 eV at zero magnetic field. For these "activated" samples ρ changes by many orders of magnitude near the IMT. In other samples (called "nonactivated") ρ varies slowly with T near room temperature and the resistivity change near the IMT is smaller. In both types of samples H_{ext} shifts the IMT to higher temperatures and makes the transition more gradual. Hall measurements show that in samples with a large IMT, the IMT is almost entirely due to a change in n, whereas in samples with a small IMT, the IMT is due to comparable changes in both n and μ. Near room temperature the Hall coefficient is H independent in the nonactivated sample, but decreases substantially with H in the activated samples. In both types of samples the Hall mobility at 298 K increases by $\sim 25\%$ when a magnetic field of 140 kOe is applied. This indicates that spin-disorder scattering is one of the main causes for the zero-field resistivity at room temperature. The various data are compared with earlier measurements by the groups at Lincoln Laboratory and at IBM, and are also discussed in terms of current theoretical models.

I. INTRODUCTION

EuO is a ferromagnetic semiconductor with a Curie temperature $T_C \cong 69$ K. The physical properties of EuO and of the other Eu chalcogenides have been the subject of numerous investigations in the last few years. The results prior to 1968 have been reviewed by Methfessel and Mattis.[1] Two extensive investigations of electrical transport in EuO by the groups at Lincoln Laboratory,[2-4] and at IBM[5-10] have been reported since then. In this paper and the following one[11] we report on measurements of the electrical resistivity and Hall effect in EuO in fields up to 150 kOe. The present work extends the earlier work on EuO and is also a continuation of our earlier electrical-transport studies in EuTe[12] and EuS[13] at high magnetic fields.

The electrical resistivity ρ of EuO is strongly influenced by the magnetic order of the localized spins of the Eu^{++} ions. The present investigation centers primarily on two phenomena which are illustrated in Fig. 1. The first of these is the rapid increase in ρ with increasing T which starts

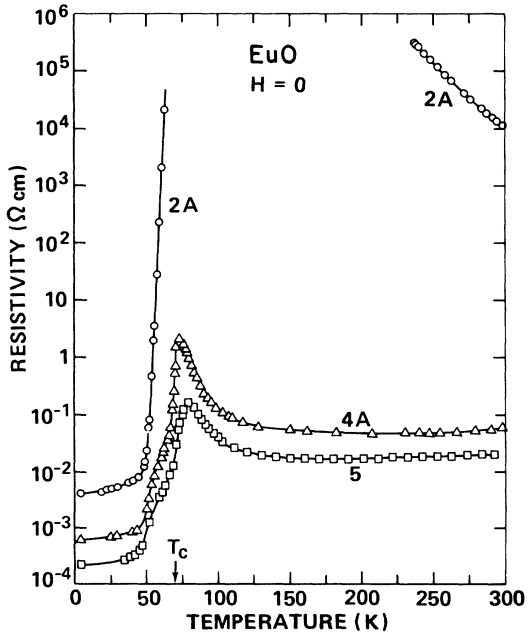

FIG. 1. Temperature variation of the zero-field resistivity of samples 2A, 4A, and 5.

TABLE I. Electrical properties of the various EuO samples.[a]

Sample No.	1	2A	2B	3	4A	4B	5
ρ(298 K) (Ω cm)	2×10^{3}	1.16×10^{4}	7×10^{4}	1.8×10^{4}	6.0×10^{-2}	5.6×10^{-2}	2.1×10^{-2}
n(298 K) (electrons/cm^3)	•••	1.9×10^{13}	•••	2.9×10^{13}	5.5×10^{18}	6.2×10^{18}	1.5×10^{19}
μ(298 K) (cm^2/V sec)	•••	29	•••	12	19	18	20
Δ_0 (eV)	~0.3	0.32 ± 0.02	0.34 ± 0.02	0.32 ± 0.01	nonactivated	nonactivated	nonactivated
ρ(4.2 K) (Ω cm)	•••	4.1×10^{-3}	•••	4.5×10^{-3}	6.3×10^{-4}	8.3×10^{-4}	2.2×10^{-4}
n(4.2 K) (electrons/cm^3)	1.7×10^{19}	1.2×10^{19}	•••	1.5×10^{19}	3.4×10^{19}	3.2×10^{19}	7.5×10^{19}
μ(4.2 K) (cm^2/V sec)	•••	1.3×10^{2}	•••	0.92×10^{2}	2.9×10^{2}	2.3×10^{2}	3.7×10^{2}
T_{max} (K)	•••	•••	•••	•••	73.4 ± 0.4	74.3 ± 0.6	79 ± 1
ρ_{max} (Ω cm)	•••	•••	•••	•••	2.1	1.0	0.16
T_c (K)	•••	69.4 ± 0.2	•••	69.8 ± 0.3	70.2 ± 0.5	71.2 ± 0.4	<72

[a] $\rho(T)$, $n(T)$, and $\mu(T)$ are the zero-field resistivity, carrier concentration, and Hall mobility, at a temperature T, respectively. The accuracy of ρ varies between 10 and 50%. The relative accuracy of ρ in a given sample, as a function of H and T, is much higher. $n(T)$ is calculated from R_0 using Eq. (2). The values for $\mu(T)=R_0(T)/\rho(T)$ are accurate to within a factor of 2. Δ_0 is the activation energy of the IMT at $T\gg T_C$, deduced from ρ vs T between 230 and 300 K. T_{max} is the temperature where the zero-field resistivity has a maximum. ρ_{max} is the zero-field resistivity at T_{max}. T_C is the Curie temperature obtained from differential susceptibility measurements.

at ~ 50 K. Earlier investigations have shown that the magnitude of this increase is strongly influenced by the stoichiometry and impurity content of the samples, which depend on the procedures of crystal growth.[2,8] In particular, samples which contain excess Eu, within certain limits (e.g., sample 2A in Fig. 1), show a change of many orders of magnitude in ρ at temperatures slightly above 50 K. This large change in ρ has been referred to as the "insulator-metal transition" (IMT).[5] In other samples, with different stiochiometry or impurity content (e.g., samples 4A and 5 in Fig. 1), the change in log ρ at temperatures slightly above 50 K is much smaller, and it appears as an "elbow" in a plot of log ρ vs. T.[2] In this paper we shall use the term IMT to describe both cases.

The resistivity near T_C could be measured only in samples with a small IMT. In these samples a second phenomenon, a resistivity peak near T_C, was observed (see Fig. 1). The procedures of crystal growth, which govern stoichiometry and impurity content, influence the magnitude of the resistivity peak and the temperature at which it occurs.[2]

An important question concerning both the resistivity peak and the IMT is to what extent the observed variation in ρ, in each case, is due to a change in the carrier concentration n and to what extent it is due to a change in the mobility μ. The direct way to answer this question is to determine n by measuring the Hall effect. However, Hall measurements on EuO are difficult to perform and their interpretation is not straightforward, for reasons discussed later. Due to these difficulties, the groups at Lincoln and at IBM used less direct methods for separating the contributions of n and μ to the resistivity ρ. One of the primary objectives of the present work was to use Hall measurements to check their conclusions directly. The present work also examines the anomalous Hall effect in EuO (or lack thereof), and the temperature at which the resistivity peak occurs. A detailed study of the temperature and magnetic field dependence of the IMT is also presented. Some aspects of this study involve magnetization and optical measurements in addition to transport measurements. The results are compared with several alternative models for the IMT.

This paper, the first of three papers, deals with

the resistivity peak and the general features of the IMT. Paper II[11] contains a more quantitative analysis of the IMT. Paper III[14] is a theoretical paper in which the two-spin correlation function of a ferromagnet is calculated as a function of magnetic field H. This theoretical calculation has a direct bearing on the discussion in Paper II.

II. EXPERIMENTAL TECHNIQUES

A. Samples

Measurements were made on seven n-type samples cleaved from five single crystals. Samples 1, 3, and 5 were obtained from three different single crystals. Samples 2A and 2B were cleaved from a fourth crystal, and samples 4A and 4B from a fifth. The five crystals were grown from Eu-rich solutions using the procedures described by Reed and Fahey.[15] The growth solution for sample No. 5 was doped with 0.1-wt% Gd_2O_3, but the concentration of Gd incorporated in sample No. 5 is not known. The other samples were not doped intentionally. Some of the physical properties of the samples are listed in Table I.

Oliver *et al.*[2] classified EuO samples into two types. Type A, grown from Eu-rich solutions, exhibited resistivity anomalies near and below T_C. Type B, grown from stoichiometric solutions, exhibited no resistivity anomalies. In terms of this classification, all our samples are type A. A more detailed classification of EuO crystals in terms of crystal-growth parameters, infrared absorption, and resistivity behavior was given by Shafer *et al.*[8] On the basis of the resistivity behavior, our samples 1, 2A, 2B, and 3 are type IV, whereas samples 4A, 4B, and 5 are type V.

The samples were rectangular parallelepipeds with typical dimensions of $1\times1\times4$ mm. In order to obtain some idea of the inhomogeneity in the carrier concentration in our samples, the Hall coefficient R in a given sample was measured several times, each time changing the position of the Hall leads. Samples 2A, 4B, and 5 were studied in this fashion. For a given sample, R did not vary by more than a factor of 1.5. The change $\Delta R/R$ as a function of magnetic field H and temperature T was very nearly independent of the position of the Hall leads. On this basis we expect that the inhomogeneity in the carrier concentration did not affect the results for the H and T variations of ρ and R. However, the inhomogeneity might have introduced an error in the values of the Hall mobility $\mu = R/\rho$ (Table I), because the values for R and ρ represented average values for different regions of the sample. In most cases the error in the absolute value of μ due to this cause was probably smaller than a factor of 1.5.

B. Electrical Measurements

Electrical leads were attached to the cleaved $\{100\}$ faces of each sample with indium solder using an ultrasonic soldering iron. Immediately before soldering, the area of the solder joint was scraped with a scalpel. Resistivity and Hall measurements were performed with a dc electric current I supplied by a Keithley model No. 225 current source. The voltage was measured with a Keithley model No. 155 microvoltmeter preceded by a Hewlett-Packard model No. 2411A guarded data amplifier, which had a much larger input impedence. The output of the microvoltmeter was fed to a recorder and could be read with a precision of $\sim 0.1\%$.

The resistivity measurements were made with a standard four-terminal arrangement. Resistivities up to $\sim 10^6\ \Omega$ cm could be measured reliably. The current I varied between 10^{-7} and 10^{-1} A and was chosen in each case to be high enough to give an easily measured resistive voltage but low enough to avoid sample heating. The resistive voltage V_R was always linear with I. Except for one case the measurements in a magnetic field were made with the external (applied) field $\vec{H}_{ext}$ perpendicular to the long axis of the sample, and hence to $\vec{I}$, i.e., $\vec{I} \parallel [100]$ and $\vec{H}_{ext} \parallel [010]$. The exceptional case is discussed in Sec. VI. In measuring the magnetoresistance, the direction of $\vec{H}_{ext}$ was reversed at each value of H_{ext}. The values of V_R for the two directions of $\vec{H}_{ext}$ were always very nearly the same, and they were averaged to obtain the final value.

Because of the finite size of the solder joints the distance between the voltage contacts could be determined only to within 10–50%, and there was a corresponding uncertainty in the *exact* value of ρ. However, the relative variation of ρ with T and H was measured with a precision of $\sim 1\%$, except in one case (Fig. 11), where the precision was 0.2%.

Hall measurements were made in all but one case with two Hall-voltage leads attached to opposite faces of the sample. The standard method of reversing $\vec{H}_{ext}$ and $\vec{I}$ was used. The major problem was the presence of a resistive voltage between the Hall leads, due to an unintentional offset of these leads. This offset problem was troublesome in cases where the resistive voltage varied rapidly with H_{ext} or with T, since in reversing the direction of $\vec{H}_{ext}$ the magnitude of H_{ext} could not be kept exactly the same and T could not be kept constant to better than ~ 0.02 K, unless the sample was immersed in a cryogenic liquid. In these cases the resistive voltage could not be eliminated entirely by reversing $\vec{H}_{ext}$. Whenever the estimated error from this source was comparable to or larger than

the Hall voltage, the Hall data were rejected. As H_{ext} increased, the Hall voltage increased faster than the offset resistive voltage. Therefore, the offset problem introduced a lower limit for the field H_{ext} at which reliable Hall data could be obtained. This lower limit varied with temperature and sample.

In one run with sample 4B the offset problem was reduced by using two voltage leads on one face of the sample and one on the opposite face. The voltage V_{12} between the first two leads was divided at $H_{ext} = 0$ in such a way that the output potential V_{out} was equal to the potential V_3 of the third lead. The voltage $(V_{out} - V_3)$ was then measured as a function of H_{ext} for both directions of $\vec{H}_{ext}$, and the Hall voltage was deduced in the standard way. This three-voltage-lead technique was not used extensively because it introduced noise problems.

C. Magnetization Measurements

Measurements of the magnetic moment versus H_{ext} were performed using two different magnetometers: a vibrating-sample magnetometer (VSM)[16] at fields below 60 kOe, and a very-low-frequency vibrating-sample magnetometer (VLFVSM)[17] in fields up to 150 kOe. In most cases the magnetization M was normalized to its saturation value M_0 measured at 4.2 K. Except at temperatures above 150 K, where the magnetization was smaller, the accuracy of M/M_0 was better than ~1%, and the precision was better than ~0.5%. The low-field susceptibility near room temperature was measured with a VSM with an accuracy of ~2%. All measurements of M were performed on the same samples which were used in the electrical measurements.

Measurements of the differential susceptibility dM/dH_{ext} were performed using an apparatus similar to the one described by Goldstein *et al.*[18] Data were taken at zero dc external magnetic field, using a modulation field with a frequency of 90 Hz and an amplitude of several Oe. Only the relative change of dM/dH_{ext} with temperature was measured by this technique.

D. Thermometry

Electrical measurements were made from 4.2 to 300 K. The samples were mounted on a copper block which could be placed inside a copper can. The temperature of the block was regulated in one of three ways: (i) by immersing the block (without the surrounding copper can) in a cryogenic liquid; (ii) by introducing He exchange gas into the surrounding can and immersing the can in a cryogenic liquid; (iii) by evacuating the can ($P \lesssim 10^{-6}$ Torr), immersing the can in a cryogenic liquid, and heating the copper block with an electrical heater to a temperature higher than that of the liquid. Liquid helium (4.2 K), liquid hydrogen (20 K), liquid nitrogen (64–78 K), liquid argon (84–88 K), and freon-11 (trichlorofluoromethane, from below 230 to 300 K) were used.

Temperatures above 20 K were measured with a platinum resistance thermometer placed inside the copper block. The electrical leads to both the thermometer and the sample were wrapped around the copper block. Thermal contact between the block, the sample, the thermometer, and the leads, was improved by using Crycon grease.[19] Corrections for the magnetoresistance of the thermometer were applied, as described earlier.[20] The temperature was measured and controlled with a precision of 0.02 K. The accuracy of the temperature measurements was better than 0.2 K. Temperatures near 4.2 and 20 K were determined by measuring the vapor pressures of the liquid helium and the liquid hydrogen, respectively.

Measurements of the magnetic moment were made in liquid helium, liquid nitrogen, liquid argon, liquid natural gas (LNG), and near room temperature. Temperatures were measured either with a copper-constantan thermocouple calibrated at the normal boiling points of liquid nitrogen and liquid argon, or with a platinum resistance thermometer. The accuracy of the temperature measurements was better than 0.2 K with the thermocouple, and better than 0.1 K with the platinum thermometer.

The differential magnetization, dM/dH_{ext}, was measured only in liquid nitrogen (64–78 K). Temperatures were measured with a platinum resistance thermometer.

E. Magnetic Fields

Most of the electrical measurements were made in a Bitter-type solenoid capable of generating magnetic fields up to 150 kOe. The magnetic field versus current characteristic of the Bitter solenoid was measured during each run with a Newport type-J integrator magnetometer,[21] which had been calibrated against an NMR probe. The accuracy of the magnetic field measurement was 0.1%, and the precision was ± 20 Oe.

When the current direction in the Bitter solenoid was reversed, keeping the magnitude of the current nominally the same, the magnitude of H_{ext} changed slightly due to a small zero offset in the current-control circuits. For this reason, the field versus current characteristic of the solenoid was measured in each run for both directions of the current, in order to correct for the small zero offset. With this correction, whenever the direction of $\vec{H}_{ext}$ was reversed the magnitude of H_{ext} was reproduced to within 100 Oe.

Some electrical measurements in fields up to 12 kOe were made in a 9-in. Varian electromagnet. The field was measured to an accuracy of better

than 0.5% with a Hall probe which had been calibrated against an NMR probe. When the direction of $\vec{H}_{ext}$ was reversed, its magnitude was reproduced to within 20 Oe.

Measurements of the magnetic moment were carried out in the following magnets: (i) a 12-in. Varian electromagnet, (ii) a 60-kOe superconducting solenoid, and (iii) a 150-kOe Bitter-type solenoid. The magnetic field produced by the Varian electromagnet was known to within 1%. With the superconducting solenoid, fields above ~40 kOe were known to within 0.3%. The field of the Bitter-type solenoid was also known to within 0.3%.[22]

F. Demagnetization Corrections

To analyze some of the data it was necessary to know the magnetic induction B inside the sample, given by $B = H_{int} + 4\pi M$. Here H_{int} is the internal magnetic field $H_{int} = H_{ext} - NM$, where H_{ext} is the external (applied) magnetic field and N is the demagnetizing factor. For an homogeneous ellipsoidal sample H_{int} and B are uniform throughout the sample. However, for the rectangular parallelepipeds used in the present work, H_{int} and B vary inside the sample.

In analyzing the electrical transport data for a particular sample it was assumed that the effect of a nonuniform B was equivalent to that of a uniform effective field $\overline{B}$. An effective demagnetization factor $\overline{N}$ was defined by the equation $\overline{B} = H_{ext} + (4\pi - \overline{N})\overline{M}$, where $\overline{M}$ was the average (measured) magnetization in the sample. It was assumed that $\overline{N}$ could be obtained by approximating the sample by an ellipsoid and using standard tables for N for ellipsoids of various shapes. The value of $\overline{N}$ obtained in this way was always close to the average demagnetizing factor N_{av} for the sample, deduced from magnetization measurements at 4.2 K (at $T \ll T_C$, $N_{av} = H_{ext}/\overline{M}$ at low fields where $\overline{M} \ll M_0$). The data for $\overline{M}(H_{ext}, T)$ used in calculating the demagnetizing corrections were obtained from magnetization measurements on the identical samples, keeping the same orientation of $\vec{H}_{ext}$ as in the transport measurements. The limitations of the above procedure for calculating the demagnetizing corrections will be discussed below whenever the resulting errors may be significant.

III. METHOD OF ANALYZING HALL DATA

The primary objective of the Hall measurements was to obtain the charge-carrier concentration n as a function of T and H. In the case of EuO the determination of n from the measured Hall voltage, V_H, is complicated by several factors which are not present in nonmagnetic semiconductors. The procedure used to obtain n from V_H is outlined below. A similar procedure was used in our earlier studies of EuTe[12] and EuS.[13]

In magnetic materials the Hall voltage is often expressed as[23]

$$V_H = (R_0 B + R_1 M)\,(I/t), \tag{1}$$

where M is the magnetization, $B = H_{int} + 4\pi M$ is the magnetic induction inside the sample, I is the electric current, and t is the thickness of the sample along the magnetic field. R_0 and R_1 are the normal (ordinary) and anomalous (extraordinary) Hall coefficients, respectively. Assuming that electrical conduction is due to carriers in a single band, the carrier concentration is given as $n = r/|R_0 e|$, where e is the charge of the electron, and r is a numerical factor of order unity. In the absence of specific information about r it is customary to set $r = 1$, so that

$$n = 1/|R_0 e|. \tag{2}$$

Equation (2), which is based on a single-band model, is also approximately valid for two conduction bands provided that the mobilities in the two bands are comparable. However, if the two mobilities are widely different, Eq. (2) will lead to erroneous results for the total electron concentration n. Two-band conduction may occur in EuO in some cases due to the spin splitting of the conduction band by the long-range magnetic order. In most of our experiments this splitting was expected to be large and only the lower-energy subband was occupied by electrons, so that the single-band model was valid. However, in a few cases the expected spin splitting was small (but nonzero) and both subbands were involved in electrical conduction. *In interpreting our Hall data we shall use Eq. (2) unless otherwise stated.* Situations where two-band conduction may play a role will be pointed out explicitly, and the effect of two-band conduction on the analysis will be considered.

The main difficulty in determining n from the measured values of V_H is that the relative contributions of the terms $R_0 B$ and $R_1 M$ to the right side of Eq. (1) are not known *a priori*. This difficulty also arises in the case of ferromagnetic metals, e.g., iron.[24] For ferromagnetic metals and alloys it is usually assumed that R_0 and R_1 are independent of H. With this assumption the coefficients R_0 and R_1 can then be determined in several ways. For example, well below T_C, V_H is linear with B at fields above magnetic saturation, since the term $R_1 M$ is then a constant. The slope of the V_H-vs-B line above magnetic saturation then gives R_0, and the extrapolated intercept of this line with the V_H axis yields R_1. In the case of EuO the assumption that R_0 is independent of H is not always justified since in some cases the carrier concentration is strongly H dependent.

In order to obtain R_0 from V_H an assumption *must* be made concerning the relative contributions

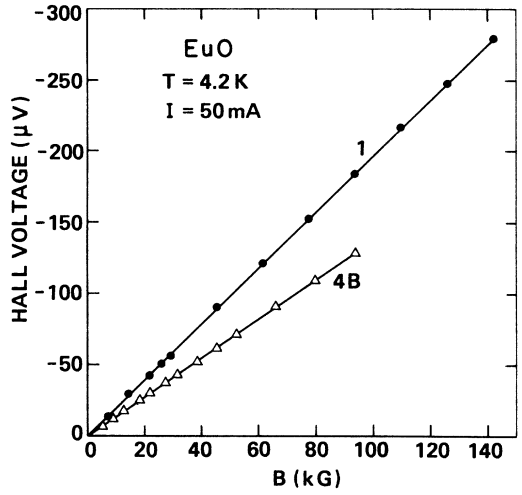

FIG. 2. Hall voltage V_H in samples 1 and 4B as a function of magnetic induction $B = H_{\text{int}} + 4\pi M$, at $T = 4.2$ K.

of the normal and anomalous Hall terms. As a guide for making a reasonable assumption we measured V_H vs B at 4.2 and 20 K. Since these temperatures are well below the IMT, n (and hence R_0) is expected to be independent of B. The results at 4.2 K for samples 1 and 4B are shown in Fig. 2. The data for V_H vs B, both below and above magnetic saturation, lie on a straight line which intersects the V_H axis near zero. Similar data were obtained for all the other samples at 4.2 K, and for sample No. 1 at 20 K. The simplest interpretation of these data is that the coefficient R_0 in Eq. (1) is independent of B at these temperatures, and that the anomalous term $R_1 M$ in Eq. (1) is very small compared to the ordinary term $R_0 B$. Thus the data at 4.2 and 20 K suggest that V_H is well approximated by the expression

$$V_H = R_0 B\,(I/t), \tag{3}$$

with no anomalous Hall term. Studies in EuS,[13] EuSe,[25] and EuTe[12] have shown that in those cases where the carrier concentration is expected to be field independent (e.g., at fields above magnetic saturation), V_H is always well approximated by Eq. (3). This indicates that in all the Eu chalcogenides $R_1 M \ll R_0 B$. In contrast, many ferromagnetic metals and alloys have a large anomalous Hall term.[24]

Based on the results at 4.2 and 20 K *we have assumed throughout this study that the Hall voltage in* EuO *is given by Eq.* (3) *at all temperatures and fields*, i.e., $R_1 M$ is always very small compared to $R_0 B$. It is important to note that we did *not* assume R_0 to be independent of either temperature or magnetic field. The carrier concentration at any temperature and field was calculated from V_H by using Eqs. (2) and (3). The Hall mobility μ was

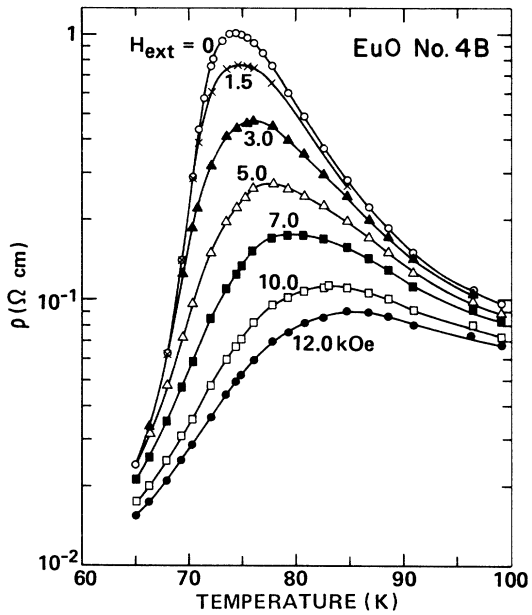

FIG. 3. T dependence of the resistivity ρ in sample 4B for various values of the external (applied) magnetic field H_{ext}.

calculated from

$$\mu = R_0/\rho. \tag{4}$$

Three additional points should be made in connection with the foregoing discussion:

(i) As stated above, the observed dependence of V_H on B at 4.2 and 20 K suggests that $R_0 B \gg R_1 M$ at these temperatures. In Sec. V C 2 we present evidence that the inequality $R_0 B \gg R_1 M$ holds at least up to ~ 55 K.

(ii) Some of the Hall data in the present work were taken near room temperature. At these temperatures $M \ll H_{\text{ext}}$, so that B is very nearly equal

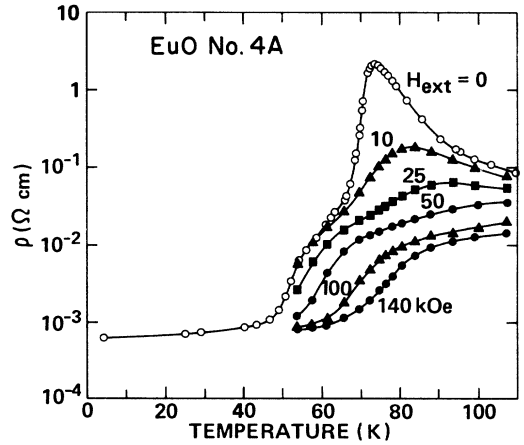

FIG. 4. T dependence of ρ in sample 4A for various values of H_{ext}.

to H_{ext}. In this case the value for R_0 deduced from V_H by using Eq. (3) is close to the value of the Hall coefficient R given by the standard formula for nonmagnetic semiconductors, viz.,

$$V_H = RH_{ext}(I/t). \tag{5}$$

(iii) The Hall voltage in magnetic materials is sometimes expressed as

$$V_H = (R_0^* H_{int} + R_1^* M)(I/t). \tag{6}$$

This expression is equivalent to Eq. (1) with $R_0^* = R_0$ and $R_1^* = R_1 + 4\pi R_0$. Users of Eq. (6) call $R_0^* H_{int}$ the "ordinary" Hall term, whereas those who use Eq. (1) call $R_0 B$ the "ordinary" term. Since Eq. (3) describes the Hall data in EuO (at least at 4.2 and 20 K), it seems natural to regard $\vec{B}$ as the effective field which governs the motion of a conduction electron in this material. This is consistent with Kittel's theoretical treatment of the motion of a conduction electron in a lattice of localized spins.[26] Although Kittel's treatment was motivated by de Haas-van Alphen results in iron, his model of a lattice of localized spins is more appropriate for the Eu chalcogenides than for iron. Throughout this paper we shall call $R_0 B$ the ordinary Hall term.

IV. RESISTIVITY PEAK

A peak in the zero-field resistivity $\rho(0, T)$ was observed in samples 4A, 4B, and 5 at a temperature near T_C. In the other four samples $\rho(0, T)$ at $T \cong T_C$ was too high to be measured with our apparatus. Hall-effect measurements were used to separate the contributions of n and μ to the peak in ρ. Since the Hall measurements require the application of a magnetic field, it is important to measure also the effect of H on the resistivity peak.

A. Effect of Magnetic Field on Resistivity Peak

The temperature variation of ρ at various fixed values of H_{ext} is shown in Figs. 3–5. Figure 3 shows the results for sample 4B in fields up to 12 kOe, and Figs. 4 and 5 show data for samples 4A and 5 at higher values of H_{ext}. As H_{ext} increases, the peak in ρ decreases, becomes broader, and shifts to higher temperatures. These general trends were observed earlier in EuO by Oliver *et al.*[2] A similar behavior was also observed in EuS (see, e.g., Ref. 13).

The effect of a magnetic field on the resistivity peak was also studied by measuring $\rho(H_{ext}, T)$ as a function of H_{ext} at fixed T. The results at 77.7 K for samples 4A, 4B, and 5 are shown in Fig. 6(a). For all three samples this temperature is within several degrees of the temperature T_{max} at which $\rho(0, T)$ is maximum. Figure 6(a) also shows that ρ decreases most rapidly with H_{ext} at low magnetic fields.

B. Hall Effect near Resistivity Peak

In Fig. 6(b) the ordinary Hall coefficient R_0 at 77.7 K is plotted as a function of H_{ext}. Reliable data below ~ 10 kOe were obtained only in sample 4B for which the resistive offset voltage was the lowest. In comparing the Hall data in Fig. 6(b) with the corresponding resistivity data in Fig. 6(a), three magnetic-field regions may be distinguished: (i) below ~ 10 kOe the data for sample 4B show that the negative magnetoresistance is due to comparable changes in $\log n$ and $\log \mu$, although the change in $\log n$ is the larger; (ii) for $10 \lesssim H_{ext} \lesssim 100$ kOe the negative magnetoresistance in all three samples is due primarily to a change in μ; (iii) above ~ 100 kOe, the data for R_0 show a slight downward curving. This downward curving is consistent with and can be related to the change of R_0 near the IMT, which is discussed in detail later. [The Hall data in Figs. 5 and 8 show that for fields between 100 and 140 kOe the IMT occurs in a temperature interval which includes 77.7 K, whereas for lower fields the IMT occurs below 77.7 K. Therefore in Fig. 6(b) the downward curving of R_0 above 100 kOe reflects, in part, the change in the carrier concentration associated with the IMT. Below 100 kOe, R_0 (77.7 K) is not affected by the IMT.] For sample 4A both μ (77.7 K) and R_0(77.7 K)

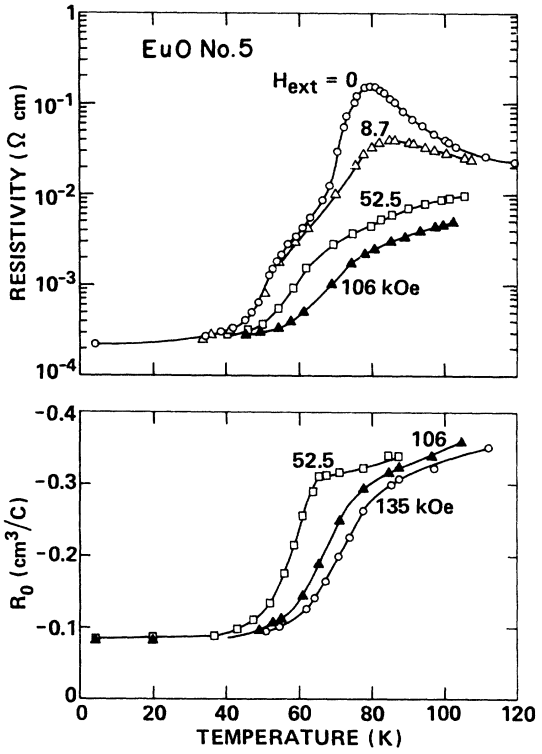

FIG. 5. T dependence of ρ and the ordinary Hall coefficient R_0 in sample 5 for various values of H_{ext}.

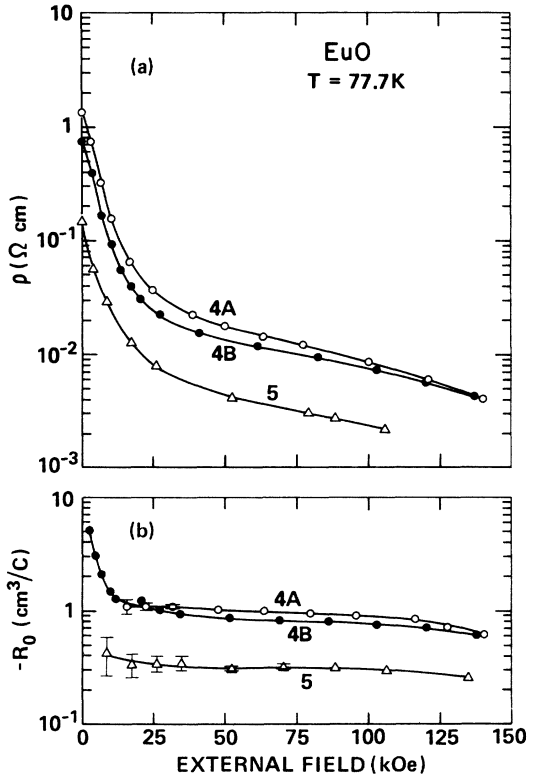

FIG. 6. Magnetic-field variation of ρ and R_0 in samples 4A, 4B, and 5 at $T = 77.7$ K. Some of the experimental uncertainties for R_0 are indicated. These uncertainties tend to decrease with increasing H_{ext}.

change by a factor of 1.4 between 100 and 140 kOe. Similar results were also obtained with sample 4B.

The temperature variation of R_0 in sample 4B between 65 and 87 K is shown in Fig. 7(a). Figure 7(b) shows the inverse Hall mobility μ^{-1} deduced from the R_0 data and the ρ-vs-T data of Fig. 3. The results in Figs. 7(a) and 7(b) show that the resistivity peak is due to changes in both n and μ. At the lowest field ($H_{ext} = 5$ kOe) the changes in n and μ make comparable contributions to the temperature variation of ρ, but as H_{ext} increases the contribution of μ becomes dominant. The value of R_0 at 65 K for $5 \leq H_{ext} \leq 10$ kOe is comparable to both the value of R_0 at 77.7 K in the region $30 < H_{ext} < 100$ kOe [see Fig. 6(b)], and to the room-temperature value $R_0 = -1.0$ cm^3/C.

Similar plots of the temperature variation of R_0 and μ^{-1} in sample 4A for $H_{ext} = 25$ kOe are shown in Fig. 8. The corresponding data for ρ are shown in Fig. 4. The increase of ρ (25 kOe, T) between 65 and 90 K is primarily due to a decrease in μ, although there is also a decrease in n.

The preceding discussion suggests that the resistivity peak at zero magnetic field is due to the combined effects of a peak in μ^{-1} and a peak in n^{-1}. The peak in n^{-1} is suppressed by applying a magnetic field of several kOe, whereas the peak in μ^{-1} is suppressed only at much higher magnetic fields. These conclusions are consistent with the *experimental results* of Oliver *et al.*,[2] but not with the discussion by the same authors in which the contribution of the peak in n^{-1} to the peak in ρ was minimized.

The peak in n^{-1} vs T, inferred from the low-field Hall data, presumably occurs because the number of conduction electrons decreases as some of them become localized. There have been several theoretical treatments of the possible localization of electrons by the magnetic interaction. Localization can take place near impurities which provide some Coulomb attraction (magnetic impurity state, or bound magnetic polaron),[27] or even in the absence of a Coulomb attraction (magnetic polaron).[9] The discussion in Ref. 9 suggests that the conditions for localization of electrons are most favorable near T_C.

The existence of a peak in μ^{-1} at temperatures near T_C can be understood qualitatively in terms of several theories for the scattering of electrons by spin fluctuations.[23,28–30] An externally applied magnetic field should reduce spin fluctuations, which would result in an increase in μ, as is observed.

It should be noted that our conclusions concerning the variation of n are based on the assumptions made in Sec. III for analysis of the Hall data. One of these assumptions was that the conduction electrons are in a single band. This assumption is

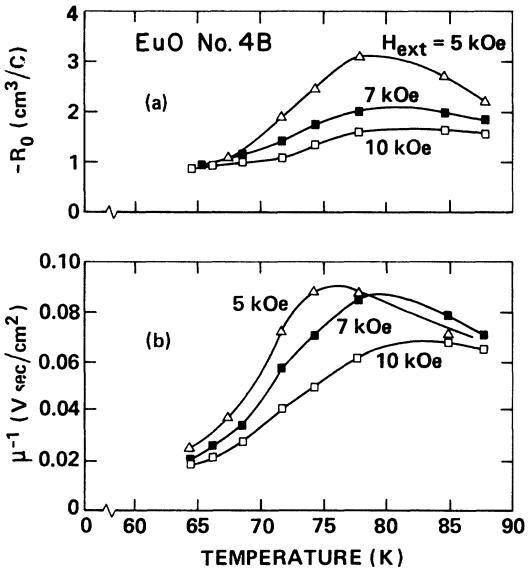

FIG. 7. T dependence of R_0 and the inverse Hall mobility μ^{-1} in sample 4B for $H_{ext} = 5$, 7, and 10 kOe. Corresponding data for ρ are shown in Fig. 3.

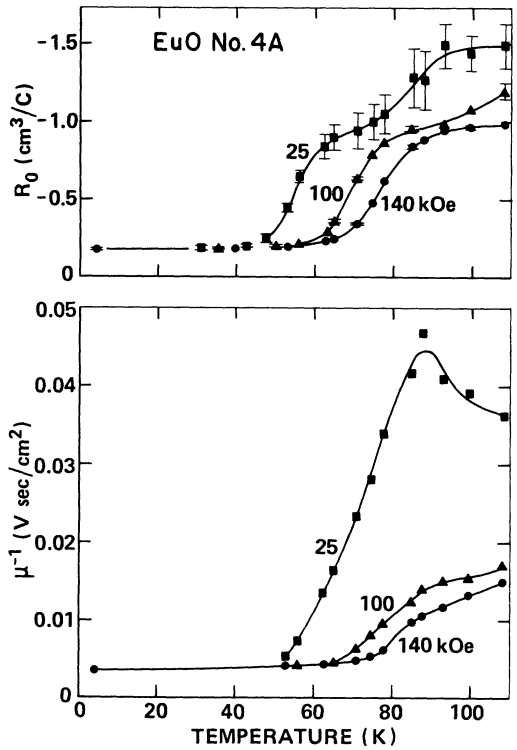

FIG. 8. T dependence of R_0 and μ^{-1} in sample 4A for $H_{ext}=25$, 100, and 140 kOe. Some of the experimental uncertainties in R_0 are indicated. Corresponding data for ρ are given in Fig. 4.

probably invalid near T_C, where, in the presence of a magnetic moment (spontaneous or field-induced), the conduction band splits into two subbands which may both contain electrons. However, unless the mobilities in the two subbands are quite different, the use of Eq. (2) to obtain n will not lead to serious errors. The other assumptions are that the anomalous Hall term is negligible and that the Hall factor r is a constant.

C. Comparison between T_{max} and T_C

According to Oliver *et al.*[2] the resistivity peak at zero applied magnetic field occurs at a temperature T_{max} which is several degrees above T_C. On the other hand, Capiomont *et al.*[31] reported that T_{max} was about 25 K below T_C in EuO films containing a large excess of Eu. In the theories of de Gennes and Friedel,[28] and of Kim[29] the magnetic scattering of electrons is dominated by long-range spin fluctuations. These theories predict that the peak in μ^{-1} is exactly at T_C. In a later paper, Fisher and Langer[30] showed that the magnetic scattering of electrons is dominated by short-range spin fluctuations and that, therefore, the peak in μ^{-1} occurs at $T>T_C$. In view of these conflicting experimental and theoretical results, we decided to measure T_C and compare it to T_{max}.

The Curie temperature of EuO depends on the impurity content and stoichiometry. For nominally pure stoichiometric samples the reported values of T_C lie between 69.2 and 69.6 K,[32–34] but values as high as 120 K have been reported for doped or nonstoichiometric samples.[2,31] Since T_C is sample dependent, a meaningful comparison between T_{max} and T_C can be made only if both temperatures are measured on the same sample.

The Curie temperature T_C was measured by three different techniques which are all based on the fact that at $T<T_C$ the low-field magnetization is limited by the demagnetizing field. Measurements of T_C were carried out on sample 4A with $T_{max}=73.4\pm0.4$ K, on sample 4B with $T_{max}=74.3\pm0.6$ K, on sample 5 with $T_{max}=79\pm1$ K, and on samples 2A and 3 for which T_{max} was not determined. The most extensive measurements were carried out on sample 4B, for which T_C was determined by all three techniques. For most of the other samples T_C was determined only by the differential susceptibility technique described below.

1. Determination of T_C by Differential Susceptibility Measurements

The differential susceptibility $(dM/dH_{ext})_0$ at zero dc applied magnetic field was measured as a function of T. Since $H_{int}=H_{ext}-NM$,

$$\left(\frac{dM}{dH_{ext}}\right)_0=\frac{\chi_0}{1+N\chi_0}\ , \tag{7}$$

where $\chi_0=(dM/dH_{int})_0$ is the differential susceptibility with respect to the *internal field*. The right-

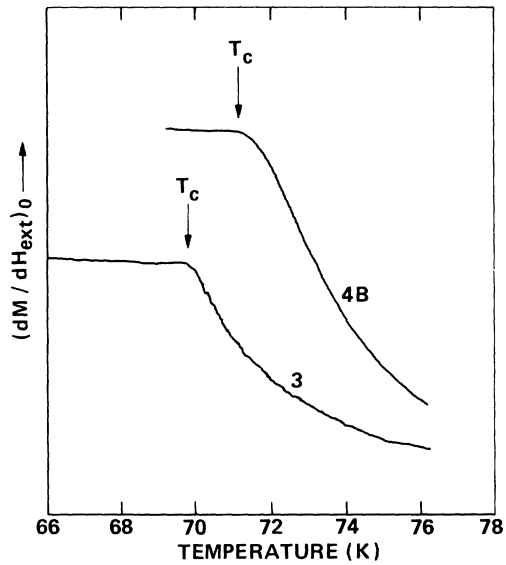

FIG. 9. Differential susceptibility $(dM/dH_{ext})_0$ vs T in samples 3 and 4B. The ordinate scale is in arbitrary units and is different for the two samples. The arrows indicate the Curie temperatures (for values and uncertainties of T_C see Table I).

hand side of Eq. (7) increases monotonically with increasing χ_0 and approaches $1/N$ as $\chi_0 \to \infty$. When the temperature of a ferromagnet decreases towards T_C, χ_0 increases. For $T \leq T_C$, $\chi_0 \gg N^{-1}$ (χ_0 is infinite in an ideal ferromagnet). Therefore, as T decreases toward T_C, $(dM/dH_{ext})_0$ first increases and then assumes the constant value $1/N$ at all temperatures below T_C. The temperature where $(dM/dH_{ext})_0$ becomes constant is T_C. In pure stoichiometric EuO samples, the temperature where $(dM/dH_{ext})_0$ becomes constant can be determined easily to within 0.2 K. For samples which contain many conduction electrons the uncertainty in T_C is larger because $(dM/dH_{ext})_0$ approaches a constant value more gradually.

Measurements of $(dM/dH_{ext})_0$ vs T were performed on several samples with room-temperature resistivities ρ_{298} from 10^{-2} to 10^4 Ω cm. The data obtained for the high-resistivity sample No. 3 and the relatively low-resistivity sample No. 4B are shown in Fig. 9. These data were taken with the modulation field $\vec{H}_{ext}$ along the long axis of each sample. Values for T_C and T_{max} are given in Table I. For the highest resistivity samples T_C was close to the values reported in the literature for pure stoichiometric EuO. For all the samples which we studied, T_C was between 69 and 72 K, where 72 K repsents an upper limit for T_C in sample 5 for which T_C could not be determined accurately. For all samples in which T_{max} was measured, T_{max} was higher than T_C.

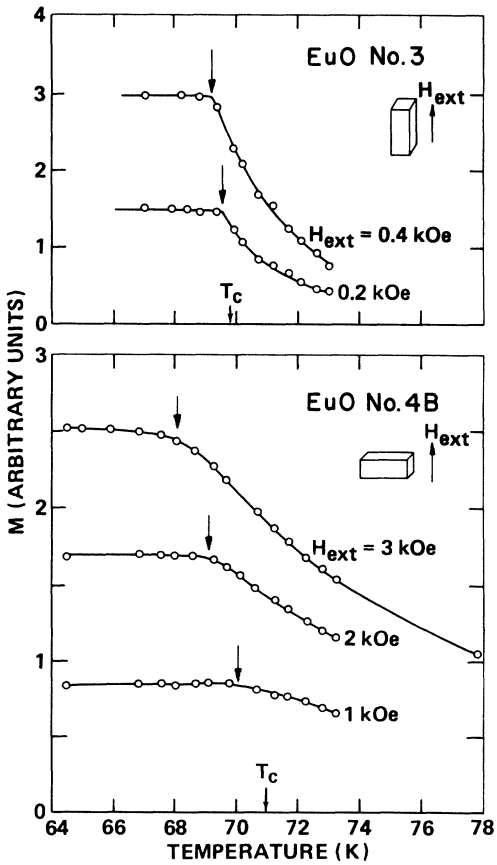

FIG. 10. T dependence of the magnetization M in samples 3 and 4B for various values of H_{ext}. The orientation of $\vec{H}_{ext}$ with respect to each sample is indicated. The arrows show the (approximate) positions of $T_K(H_{ext})$ and the extrapolated values of T_C.

2. Determination of T_C by Magnetization Measurements

To determine T_C from magnetization measurements we used a method first proposed by Rayl and Wojtowicz[35] and used on EuO by Menyuk *et al.*[32] This method utilizes the fact that the M-vs-T curve, for a low fixed H_{ext}, exhibits a kink at a temperature $T_K(H_{ext})$. For a given H_{ext} the magnetization at $T < T_K$ is constant (equal to H_{ext}/N) but above T_K, M decreases rapidly with T. T_C is obtained by extrapolation of the curve for $T_K(H_{ext})$ vs H_{ext} to $H_{ext} = 0$.

Results for M vs T in samples 3 and 4B, for various values of H_{ext}, are shown in Fig. 10. The orientation of $\vec{H}_{ext}$ relative to each sample is indicated in this figure. The demagnetizing factor N is much smaller when $\vec{H}_{ext}$ is parallel to the long axis of the sample, which results in a sharper kink in the M-vs-T curve. These measurements gave $T_C = 71 \pm 1$ K for sample 4B, in agreement with the value $T_C = 71.2 \pm 0.4$ obtained from measurements of $(dM/dH_{ext})_0$. Measurements of M vs T on sample 3 gave $T_C = 69.8 \pm 0.5$ K, in good agreement with $T_C = 69.8 \pm 0.3$ K obtained from measurements of $(dM/dH_{ext})_0$.

3. Determination of T_C by Magnetoresistance Measurements

In a conducting sample the carrier concentration may be inhomogeneous resulting in a variation of T_C inside the sample. In this case the value of T_C obtained from the two magnetic methods described above may not be representative of the more conducting parts of the sample which govern the resistivity behavior. Since T_{max} is determined from resistivity measurements, a more meaningful comparison between T_{max} and T_C is obtained if T_C is also determined from the resistivity.

The principle of determining T_C from magnetoresistance measurements is illustrated by the results in Fig. 11 where the ratio $\rho(H_{ext})/\rho(0)$ for sample 4B is plotted versus T for two values of H_{ext}. For each value of H_{ext} the negative magnetoresistance disappears abruptly at a temperature marked by an arrow. This temperature is close to the value of $T_K(H_{ext})$ in the lower part of Fig. 10 (the data in Fig. 11 and the lower part of Fig. 10 were taken with the same orientation of $\vec{H}_{ext}$ relative to the sample).

The results in Fig. 11 can be explained if one

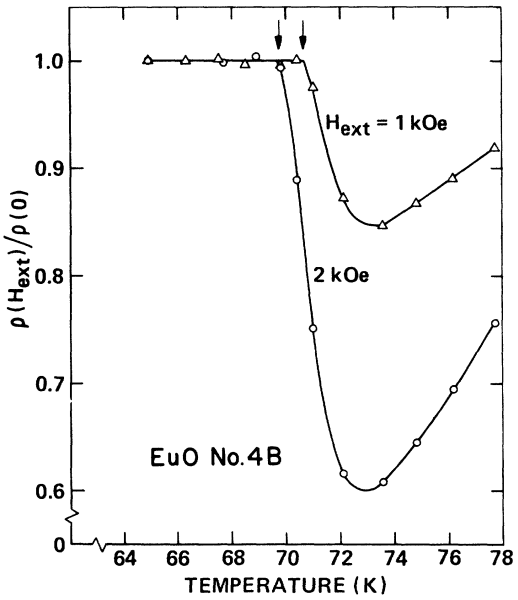

FIG. 11. T dependence of the ratio $\rho(H_{ext})/\rho(0)$ in sample 4B for $H_{ext}=1$ and 2 kOe. The arrows indicate the temperatures at which $\rho(H_{ext})/\rho(0)$ becomes equal to 1.

assumes that the magnetoresistance is determined by the internal field, H_{int}. For each value of H_{ext} smaller than NM_0 there is a temperature below which $H_{int}=0$. This temperature is $T_K(H_{ext})$, as defined in the discussion of the magnetization measurements. Consequently the negative magnetoresistance disappears when the temperature is below $T_K(H_{ext})$. Extrapolating $T_K(H_{ext})$ vs H_{ext} to $H_{ext}=0$ gives T_C. It is clear that this method of determining T_C is similar to that in Sec. IV C 2, except that $T_K(H_{ext})$ is determined from ρ rather than from M. (See *Note added in proof.*)

Measurements of $\rho(H_{ext})/\rho(0)$ were carried out on sample 4B for $H_{ext}=0.2$, 0.5, 1.0, 1.5, and 2.0 kOe. The results in all fields were similar to those shown in Fig. 11. A value $T_C=71.5\pm0.7$ K was obtained from these data. This value, which is close to those obtained from measurements of M and $(dM/dH_{ext})_0$, is lower than T_{max}.

4. Conclusion

For all samples in which both T_{max} and T_C were determined, T_{max} was several degrees higher than T_C. This result agrees with that of Oliver *et al.*[2] and is also consistent with the theory of Fisher and Langer.[30]

V. INSULATOR-METAL TRANSITION (IMT)

A. Model for the IMT

The present understanding of the IMT is based on a model which was proposed by Oliver *et al.*[2-4] and modified later by several authors.[5,6,9,10,36] A similar model was introduced earlier by Lehmann[37] to explain the behavior of n-type $CdCr_2Se_4$. Since much of the following discussion is based on this model, we review its main features below.

1. Basic Model

In EuO there is a large interaction between the spin of an electron in the conduction band and the spins of the Eu^{++} ions. Due to this interaction the energy of the conduction-band edge depends on the magnetic order, and therefore on T and H. Moreover, below T_C this interaction splits the conduction band into two subbands: a lower subband for electrons with spins parallel to the net magnetization, and a higher subband for electrons with spins in the opposite direction.[38] These effects of the magnetic order on the conduction band are shown schematically in Fig. 12. One consequence of the lowering of the conduction-band edge with increasing magnetic order is that the optical absorption edge shifts to longer wavelengths with decreasing temperature. This so-called red shift has been observed in EuO by several investigators.[39]

The main assumption of the model for the IMT is that this transition is due to the presence of electron traps which at $T \gg T_C$ are located a few tenths of an eV below the conduction-band edge. In their original model, Oliver *et al.* postulated that the energy of a trapped electron did not depend on magnetic order. Although this assumption has been modified in later versions of the model, many of the basic features of the model are not altered by these modifications. For the moment we shall

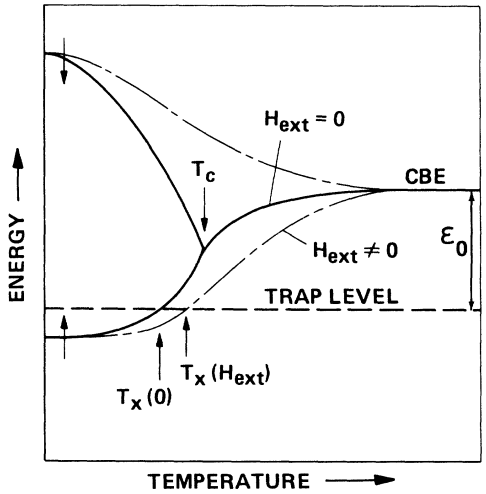

FIG. 12. Schematic energy-level diagram showing the basic features of the model for the IMT. The shift and splitting of the conduction-band edge (CBE) with temperature for both $H_{ext}=0$ and $H_{ext}\neq 0$ are indicated. The trap level is represented by horizontal dashed line. T_x is the temperature where the conduction-band edge crosses the trap level. ϵ_0 is the energy separation between the CBE and the trap level at high temperatures.

assume a trap level which does not depend on magnetic order. This trap level is represented by a dashed horizontal line in Fig. 12.

As shown in Fig. 12, the conduction-band edge moves below the trap level as T decreases. The crossing of the trap level and the conduction-band edge occurs at a temperature T_x which is lower than T_C. This level crossing at T_x results in a transfer of electrons from the traps to the conduction band for decreasing T, and *vice versa* for increasing T. The change in the carrier concentration n in the conduction band produces the large change in ρ which is the IMT.

The shape of the ρ-vs-T curve depends on whether the trap concentration N_t is larger or smaller than the total concentration N_e of electrons which are potentially available for electrical conduction. If $N_t > N_e$, then conduction at $T \gg T_C$ is due to the relatively small concentration n of electrons thermally excited from the trap level to the conduction band. At these high temperatures $\rho(T) \sim e^{\Delta_0/kT}$, where Δ_0 is an activation energy which depends on the energy separation ϵ_0 between the trap level and the conduction-band edge at $T \gg T_C$. There are two limiting situations[40]: (i) If there are enough compensating acceptors, the Fermi level is pinned close to the trap level, and $\Delta_0 = \epsilon_0$. Penney *et al.*[5] have argued that this is the case for samples with $\Delta_0 \cong 0.3$ eV. (ii) In the absence of acceptors, the Fermi level is approximately halfway between the trap level and the conduction-band edge, so that $\Delta_0 = \frac{1}{2}\epsilon_0$.

In the opposite case when $N_t < N_e$, there is always a concentration of at least $(N_e - N_t)$ electrons in the conduction band. In this case $\rho(T)$ does not vary exponentially with T at $T \gg T_C$, except at very high temperatures where the concentration of thermally excited electrons becomes comparable to $N_e - N_t$. In addition, the change in log n at temperatures near T_x will be smaller in the case $N_t < N_e$ than in the case $N_t > N_e$, so that samples with $N_t < N_e$ exhibit a small IMT (resistivity "elbow") rather than a large IMT.

2 *Refinements of the Model*

Since Oliver *et al.*[2-4] introduced the trap model, several modifications and refinements of the model have been proposed. These refinements do not alter the basic feature of the model, which is that the IMT results from a crossing of a trap level and the conduction-band edge. The various modifications and refinements can be grouped into three categories:

a. Nature of the trap. The assumption that the energy of the trapped electrons is independent of magnetic order implies that these electrons are completely localized at the trap sites.[23] The complete localization of the trapped electrons was questioned by von Molnar and Kasuya.[9] Instead, they proposed that the traps are oxygen vacancies. Each vacancy acts as a center with a positive charge $+2|e|$, which can trap two electrons. The electronic ground state of the two trapped electrons is similar to that of the He atom, i.e., two electrons in the $1s$-orbital state, one with spin up and the other with spin down ($1s\uparrow 1s\downarrow$). The same model for the trap was also proposed independently by Oliver *et al.*[2] The suggestion that the traps are oxygen vacancies is supported by studies of the dependence of the IMT on the stoichiometry of the EuO samples.[2,8] Later, Torrance *et al.*[10] argued that the electronic ground state near an oxygen vacancy is not similar to that of the He atom, and that instead it can be described as a bound magnetic polaron. In this model the exchange interaction between the electrons and the Eu^{++} ions plays an important role in determining the binding energy of trapped electrons. Very recently the influence of the exchange interaction on the binding energy of an electron near a hydrogenic impurity has been considered by Leroux-Hugon.[36] His treatment differs from other treatments in that the dependence of the binding energy on the electron concentration is considered. According to his analysis the IMT should occur only for a relatively narrow range of N_e. It should be noted that the calculations by Leroux-Hugon for hydrogenic impurities, each with $+|e|$ charge, may not apply directly to EuO because the traps in this material are probably oxygen vacancies.

The various ideas summarized in the last paragraph suggest that at present the exact nature of the electronic ground state of the trap is still open to discussion.

b. Excited states of electrons near the trap. Petrich *et al.*[6] and Penney *et al.*[5] have discussed the excited states of electrons near the traps. If one assumes that the traps are oxygen vacancies with a ($1s\uparrow 1s\downarrow$) electronic ground state, then the first excited state is a triplet state ($1s\uparrow 2s\uparrow$) with a net spin of 1. When long-range magnetic order is present, the triplet state will split into three levels. Moreover, due to the random distribution of traps there will be some spread in the energy of the excited states. Excited states with sufficiently high energy may mix with conduction-band states. This picture was invoked by Petrich *et al.*[6] to interpret their results on the isomer shift in Eu-rich EuO samples which show an IMT.

c. Dependence of the activation energy Δ on magnetic order. The shape of the logρ-vs-T curve in samples with $N_t > N_e$ is determined primarily by the dependence of the energy separation between the trap level and the conduction-band edge on magnetic order. Several proposals for this dependence have been advanced.[2,5] This topic is discussed in detail in the following paper.[11]

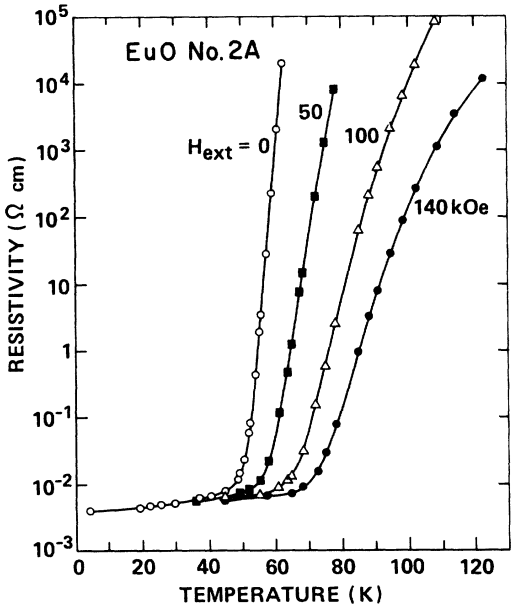

FIG. 13. IMT in sample 2A at $H_{ext} = 0$, 50, 100, and 140 kOe.

B. Dependence of the IMT on H_{ext}

Figure 1 shows that some of our samples had a very large IMT, whereas others had a relatively small IMT (resistivity "elbow"). In terms of the trap model of Sec. V A the large IMT corresponds to $N_t > N_e$, and the small IMT corresponds to $N_t < N_e$. As shown later in Sec. VI, this interpretation is consistent with the results near room temperature.

The effect of an external magnetic field on the IMT is shown in Figs. 4 and 5 for samples with a small IMT, and in Figs. 13 and 14 for samples with a large IMT. Two features should be noted: (i) As H_{ext} increases, the IMT shifts to higher temperatures. (ii) The increase of $\log\rho$ with increasing T becomes more gradual as H_{ext} increases. These two features were observed earlier by Oliver *et al.*[2] who studied the IMT in magnetic fields up to 48 kOe. These authors pointed out that both features can be explained by the trap model. For example, the shift of the IMT to higher temperatures with increasing H_{ext} is attributed to the increase of magnetic order with increasing H_{ext}. As shown in Fig. 12, a magnetic field lowers the conduction-band edge and therefore increases the temperature T_x at which the conduction-band edge crosses the trap level.

A detailed analysis of the resistivity data in Figs. 13 and 14 will be presented in the following paper.[11] Here, we only point out the striking similarity between these two sets of data for samples from different single crystals.

C. Hall Effect near IMT

To determine the variation of n and μ near the IMT, the Hall voltage V_H was measured as a function of T at fixed values of H_{ext}. The Hall data were analyzed by the method described in Sec. III, using magnetization data to obtain the values of the magnetic induction B inside the sample. The values of R_0 obtained from this analysis were then used to determine n by means of Eq. (2). Values of μ were calculated from the values of R_0 and the resistivity ρ by using Eq. (4).

1. Changes of n and μ near IMT

The Hall measurements were carried out on samples 2A and 3 ($N_t > N_e$), and on samples 4A and 5 ($N_t < N_e$) in fields up to 140 kOe. In the latter samples the resistivity changed by only one order of magnitude near the IMT (see Figs. 4 and 5). The separate contributions of n and μ to the IMT in sample 4A are shown in Fig. 8 where R_0 and μ^{-1} are plotted against temperature. For $H_{ext} = 140$ kOe the IMT occurs between ~ 60 and ~ 90 K. In this temperature range R_0 (140 kOe) increases by a factor of 4.2 and μ (140 kOe) decreases by a factor 2.5. For $H_{ext} = 100$ kOe, the IMT occurs between ~ 55 and ~ 85 K where R_0 increases by a factor of 4.1 and μ decreases by a factor of 3.0. For $H_{ext} = 25$ kOe, the IMT occurs between ~ 45 and ~ 65 K, where R_0 increases by a factor of 4.2 and μ decreases by a factor of 4.1.

The above results for sample 4A show that (i) the change in $\log n$ and $\log\mu$ near the IMT are comparable, although the change in $\log n$ is somewhat

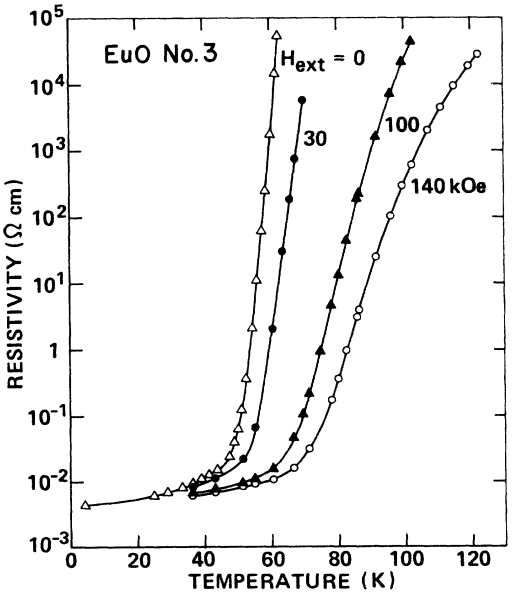

FIG. 14. IMT in sample 3 at $H_{ext} = 0$, 30, 100, and 140 kOe.

larger. Oliver *et al.* arrived at a similar conclusion for comparable samples (see Fig. 10 of Ref. 2). (ii) The change in n near the IMT is nearly the same for all values of H_{ext}. This result is consistent with the trap model of Sec. V A. According to this model, if $N_t < N_e$ then $n \cong N_e$ at $T < T_x$ (H_{ext}), and $n \cong (N_e - N_t)$ at $T \gg T_x$ (H_{ext}), for all values of H_{ext}. Therefore, the change in n near the IMT is approximately equal to N_t for all H_{ext}. (iii) The change in μ near the IMT, for a fixed H_{ext}, decreases as the value of H_{ext} increases. A possible explanation of this effect is that the low-temperature "tail" of the resistivity peak overlaps the high temperature part of the IMT. Consequently, some of the mobility variation near the IMT reflects the mobility changes associated with the resistivity peak (see the curve for μ^{-1} at $H_{ext} = 25$ kOe in Fig. 8). Since the resistivity peak decreases rapidly with H_{ext}, the mobility change due to the "tail" of the resistivity peak decreases with H_{ext}.

Results for ρ and R_0 in sample 5 are shown in Fig. 5. These results are similar to those in sample 4A, and lead to similar conclusions.

In samples 2A and 3 the resistivity changed by many orders of magnitude near the IMT. The variation of R_0 with T in sample No. 3 for $H_{ext} = 100$ and 140 kOe, is shown in Fig. 15. Also shown in Fig. 15 is the apparent Hall mobility $\mu_{app} = R_0/\rho$. The word "apparent" is used for the following reason. Both ρ and R_0 are sensitive to a change in B, where $B = H_{ext} + (4\pi - N)M$. The field B is nonuniform in a nonellipsoidal sample. Since the resistivity and Hall data were taken with different sets of voltage leads, it is possible that the effective demagnetizing factor was not identical in both cases. This means that for the same H_{ext} the magnetic induction B may have been slightly different for the two sets of data. Therefore, the true Hall mobility μ may be different from μ_{app}. This difference can be estimated from the dependence of ρ on H_{ext} and the fact that two demagnetizing factors cannot differ by more than 4π. Assuming a difference of 4π between the two values of N one obtains a maximum possible difference of a factor of 10 between μ_{app} and μ. More realistically, the difference between the two effective demagnetizing factors probably did not exceed 3, and μ_{app}/μ was probably between $\frac{1}{2}$ and 2. In samples 4A, 4B, and 5, μ_{app} was closer to μ because ρ and R_0 were less sensitive to a change in B than in samples 2A and 3.

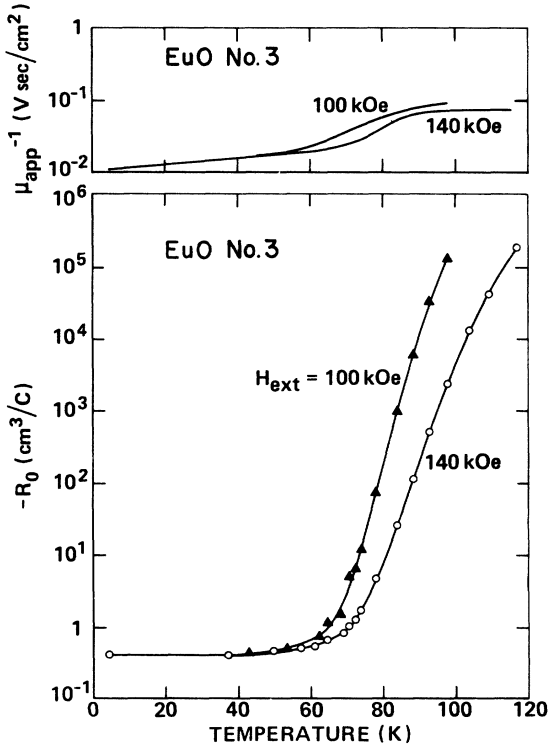

FIG. 15. T dependence of R_0 in sample 3 at $H_{ext} = 100$ and 140 kOe (lower part). The upper part of the figure shows the T dependence of μ_{app}^{-1} for the same fields (for a definition and a discussion of μ_{app} see text). Corresponding data for ρ are shown in Fig. 14.

From Fig. 15 it is clear that *the IMT in sample No. 3 is due almost entirely to a change in n.* This conclusion agrees with the results of Oliver *et al.* for samples with a large IMT (see Figs. 4 and 6 of Ref. 2).

Hall data on sample 2A, taken at 100 and 140 kOe, gave similar results to those obtained with sample No. 3.

Concerning the small variation of μ near the IMT of sample 3, it should be noted that the change in $\log\mu$ was comparable to that found in samples 4A and 5, which had a much smaller IMT (compare Figs. 8 and 15 for 100 and 140 kOe). Owing to experimental difficulties, the variation of R_0 and μ in magnetic fields well below 100 kOe could not be measured in sample No. 3. However, the results in samples 4A and 5 show that the change in $\log\mu$ near the IMT was larger at low fields, apparently because the low-temperature tail of the resistivity peak overlapped the high-temperature part of the IMT. Although no low-field Hall data were taken for samples 2A and 3, we expect that also in these samples the change in $\log\mu$ near the IMT would be larger at low fields than at high fields.

To summarize, we find that in samples with a large IMT, the IMT is due almost entirely to a change in n. In samples with a relatively small IMT (one order of magnitude change in ρ) the changes in $\log n$ and $\log\mu$ near the IMT are comparable, although the change in $\log n$ is slightly larger. The change of $\log\mu$ near the IMT, for a fixed H_{ext}, increases as the value of H_{ext} decreases.

At zero and low magnetic fields the low-temperature tail of the resistivity peak may overlap the high-temperature part of the IMT, which makes the separation of the two phenomena difficult.

2. *Comment Concerning the Anomalous Hall Effect*

From the trap model for the IMT one expects that for a given H_{ext}, $n(H_{ext}, T)$ is temperature independent at $T < T_x(H_{ext})$. This conclusion agrees with the results for R_0, which show that at temperatures below the IMT, R_0 is temperature independent (see Figs. 5, 8, and 15).

The preceding argument can be inverted in order to evaluate the importance of the anomalous Hall effect at temperatures up to ~ 55 K. It was shown in Sec. III that $R_1 M \ll R_0 B$ at 4.2 and 20 K. Suppose now that R_1 increases with T and that $R_1 M$ becomes comparable to or larger than $R_0 B$ at some temperature between 20 and ~ 55 K. If this were the case, then Eq. (3) would not be valid. The erroneous use of Eq. (3) would then lead to values for $R_0(H_{ext}, T)$ that would vary with T at temperatures below $T_x(H_{ext})$, unless the carrier concentration $n(H_{ext}, T)$ changes with T in such a way that the change of $R_0 B$ exactly cancels the term $R_1 M$ in Eq. (1). Such a fortuitous cancellation in all samples is unlikely. Furthermore, the trap model for the IMT predicts that $n(H_{ext}, T)$ is temperature independent below $T_x(H_{ext})$. The fact that Eq. (3) led to values for $R_0(H_{ext}, T)$ which were temperature independent below $T_x(H_{ext})$ is therefore a strong indication that $R_1 M \ll R_0 B$ for all temperatures below $T_x(H_{ext})$. At 140 kOe, $T_x \gtrsim 55$ K so that $R_1 M$ is small below ~ 55 K.

VI. MAGNETORESISTANCE AND HALL EFFECT AT $T \gg T_C$

Although the IMT at $H = 0$ occurs below T_C, some important information concerning the IMT can be obtained from measurement at $T \gg T_C$. For convenience, the measurements of $R(H)$ and $\rho(H)$ were carried out between 230 and 300 K, that is, at $T \sim 4T_C$.

According to the trap model of Sec. V A, the qualitative behavior of ρ at $T \gg T_C$ depends on whether $N_e > N_t$ or $N_e < N_t$. When $N_e > N_t$ the concentration n of charge carriers in the conduction band at $T \gg T_C$ is approximately equal to $(N_e - N_t)$. In such samples ρ varies relatively slowly with T at $T \gg T_C$, i.e., electrical transport at these temperatures is not governed by an activation energy and $\rho(T)$ does not vary exponentially with T. Samples 4A, 4B, and 5 fall into this category. We shall refer to these samples as "nonactivated".

When $N_e < N_t$ electrical conduction at $T \gg T_C$ is due primarily to carriers which are thermally excited from the trap level to the conduction band. In this case n is proportional to $e^{-\Delta/kT}$, where $\Delta(H, T)$ is an activation energy. The *zero-field* resistivity at $T \gg T_C$ is governed by the activation energy $\Delta_0 \equiv \Delta(H = 0, T \gg T_C)$, i.e., $\rho(T) \sim e^{\Delta_0/kT}$. We shall refer to such samples as "activated". Examples are samples 1, 2A, 2B, and 3. Values of Δ_0 for these samples are given in Table I. These values were obtained from the temperature dependence of the zero-field resistivity between 230 and 300 K. The Hall measurements on samples 2A and 3 showed that the exponential variation of ρ with T was due to a change in n, as expected. For example, in sample 3 the T dependence of ρ gave $\Delta_0 = 0.32 \pm 0.01$ eV, whereas the T dependence of n, at $H = 0$, gave $\Delta_0 = 0.34^{+0.04}_{-0.02}$ eV.

The application of a magnetic field causes an increase in both the long-range and short-range magnetic order. For example, at $T \cong 4T_C$ a field of 150 kOe increases the reduced magnetization $\sigma = M/M_0$ from zero to ~ 0.15. For activated samples the H-induced increase in the magnetic order decreases Δ, which results in an increase of n and a corresponding decrease of ρ. On the other hand, in nonactivated samples n is expected to be very nearly H independent ($n \cong N_e - N_t$). There still can be an H-induced change in ρ in the nonactivated samples due to a change of μ with H. However, this magnetoresistance should be smaller than in the activated samples because in the latter samples *both* n and μ vary with H.

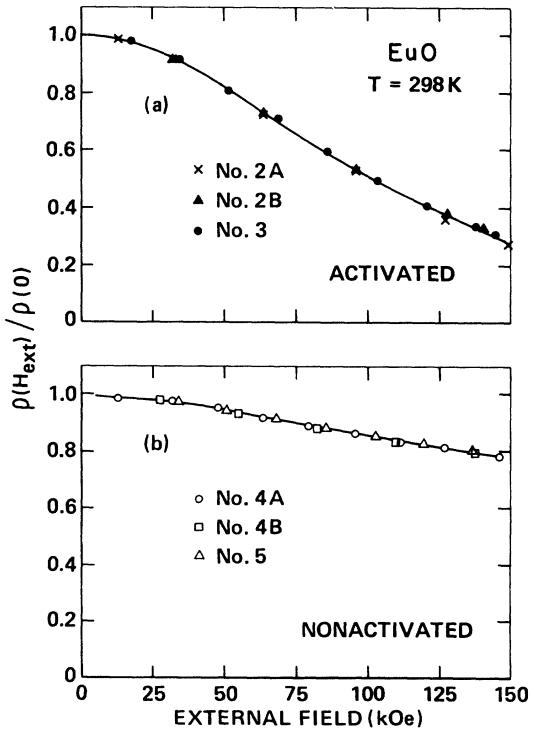

FIG. 16. $\rho(H_{ext})/\rho(0)$ vs H_{ext} at $T = 298$ K. (a) Activated samples. (b) Nonactivated samples. In both cases $\vec{I} \parallel [100]$, $\vec{H}_{ext} \parallel [010]$.

The H dependence of ρ at 298 K for activated and nonactivated samples is shown in Figs. 16(a) and 16(b), respectively. The values of $\rho(H_{ext})/\rho(0)$ for all the activated samples fall on one curve, and those for all the nonactivated samples fall on another. It is clear that the negative magnetoresistance in the activated samples is larger than in the nonactivated samples, as expected. Additional measurements on sample 2A (activated) showed that $\rho(H)/\rho(0)$ depends only on the magnitude of $\vec{H}$ but not on its direction relative to the crystallographic axes.

The H dependence of the Hall coefficient R for one activated and two nonactivated samples at 298 K is shown in Fig. 17.[41] In the activated sample $|R|$ decreases appreciably with H_{ext}, whereas in the nonactivated samples R is independent of H_{ext} within the experimental uncertainties. Both of these results are in accord with the trap model of Sec. *V A*. A detailed analysis of the Hall effect in the activated samples is given in the following paper.[11]

The H dependence of the Hall mobility μ at 298 K is shown in Fig. 18. These results were obtained from the data in Figs. 16 and 17. Note that $\mu(H_{ext})/\mu$ (140 kOe) is similar for both activated and nonactivated samples. At 140 kOe, μ is about 25% higher than at $H_{ext} = 0$. Since at 298 K the reduced magnetization at 140 kOe is only ~ 0.13, it is likely that a higher degree of spin alignment produced by a stronger magnetic field would result in a further increase in μ. This suggests that at 298 K there is a substantial magnetic contribution to the scattering of electrons at zero field. Kasuya[42] and others[29] have shown that the scattering of electrons by the spins of the magnetic ions does not vanish above T_C, and that even at $T \gg T_C$ the scattering due to spin disorder leads to a finite resistivity. Qualitatively, the application of a magnetic field should lead to an increase in μ. The H-induced increase in μ was calculated for some cases by Haas.[43]

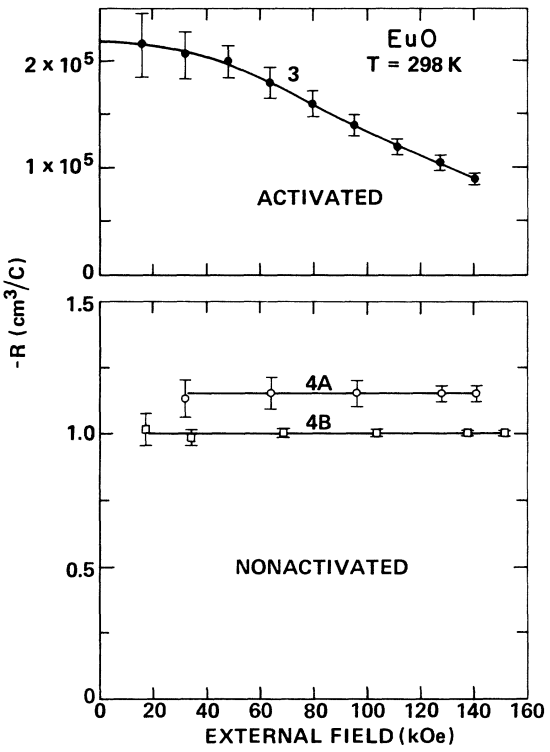

FIG. 17. Hall coefficient R vs H_{ext} at 298 K. Upper part is for sample 3 (activated). Lower part is for samples 4A and 4B (nonactivated). See Ref. 41.

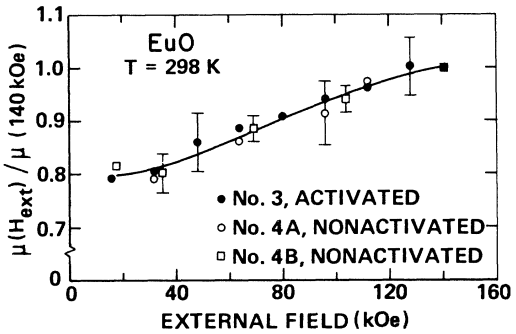

FIG. 18. Variation of the Hall mobility μ with H_{ext} at 298 K. The data for each sample were normalized to the value of μ at $H_{ext} = 140$ kOe. Sample 3 is activated, whereas samples 4A and 4B are nonactivated. Some typical experimental uncertainties are indicated.

Since a sizable fraction of the resistivity at $H = 0$ is apparently due to magnetic scattering, it is unlikely that the room-temperature mobility of EuO samples will increase substantially when crystals with a higher degree of perfection become available.

In summary, the mobility at $T \sim 4T_C$ appears to be influenced by magnetic scattering and it increases with H, as expected. The H dependence of R in both activated and nonactivated samples is explained (at least qualitatively) in terms of the trap model. A quantitative analysis of the Hall data is given in the following paper,[11] which discusses the dependence of Δ on magnetic order.

Note added in proof. For analogous results for the tunneling conductance in EuS, see Thompson *et al.*, AIP Conf. Proc. 5, 827 (1971), Fig. 3.

ACKNOWLEDGMENTS

The authors wish to thank Dr. A.J. Strauss for detailed comments concerning the manuscript. We are also indebted to Dr. M.R. Oliver and Dr. H. C. Praddaude for useful discussions. We are grateful to E. J. McNiff, Jr. for collaboration in the high-field magnetization measurements, to R. E. Fahey for assistance in the crystal-growth work, and to V. Diorio for technical assistance in the transport measurements.

*Supported by the National Science Foundation.
†Work sponsored by the Department of the Air Force.

[1]S. Methfessel and D. C. Mattis, in *Handbuch der Physik*, edited by S. Flügge (Springer-Verlag, Berlin, 1968), Vol. 18, Pt. I.
[2]M. R. Oliver, J. O. Dimmock, A. L. McWhorter, and T. B. Reed, Phys. Rev. B **5**, 1078 (1972).
[3]M. R. Oliver, J. O. Dimmock, and T. B. Reed, IBM J. Res. Dev. **14**, 276 (1970).
[4]M. R. Oliver, J. A. Kafalas, J. O. Dimmock, and T. B. Reed, Phys. Rev. Lett. **24**, 1064 (1970).
[5]T. Penney, M. W. Shafer, and J. B. Torrance, Phys. Rev. B **5**, 3669 (1972).
[6]G. Petrich, S. von Molnar, and T. Penney, Phys. Rev. Lett. **26**, 885 (1971).
[7]S. von Molnar and M. W. Shafer, J. Appl. Phys. **41**, 1093 (1970).
[8]M. W. Shafer, J. B. Torrance, and T. Penney, AIP Conf. Proc. **5**, 840 (1972); and J. Phys. Chem. Solids **33**, 2251 (1972); F. Holtzberg, T. R. McGuire, T. Penney, M. W. Shafer, and S. von Molnar, IBM Technical Report, June, 1971 (unpublished).
[9]S. von Molnar and T. Kasuya, in *Proceedings of the Tenth International Conference on the Physics of Semiconductors, Cambridge, Mass., 1970* (U.S. Atomic Energy Commission, Oak Ridge, Tenn., 1970), p. 233.
[10]J. B. Torrance, M. W. Shafer, and T. R. McGuire, Phys. Rev. Lett. **29**, 1168 (1972).
[11]Y. Shapira, S. Foner, R. Aggarwal, and T. B. Reed, following paper, Phys. Rev. B **8**, 2316 (1973).
[12]Y. Shapira, S. Foner, N. F. Oliveira, Jr., and T. B. Reed, Phys. Rev. B **5**, 2647 (1972).
[13]Y. Shapira and T. B. Reed, Phys. Rev. B **5**, 4877 (1972).
[14]H. Birecki, H. E. Stanley, and Y. Shapira, second following paper, Phys. Rev. B 8, 2327 (1973).
[15]T. B. Reed and R. E. Fahey, J. Cryst. Growth **8**, 337 (1971).
[16]S. Foner, Rev. Sci. Instrum. **30**, 548 (1959).
[17]S. Foner and E. J. McNiff, Jr., Rev. Sci. Instrum. **39**, 171 (1968).
[18]A. Goldstein, S. J. Williamson, and S. Foner, Rev. Sci. Instrum. **36**, 1356 (1965).
[19]Manufactured by Air Products and Chemicals, Allentown, Pa.
[20]L. J. Neuringer, A. J. Perlman, L. G. Rubin, and Y. Shapira, Rev. Sci. Instrum. **42**, 9 (1971).
[21]Manufactured by Newport Instruments, Newport Pagnell, England.
[22]The uncertainty of 0.3% in H_{ext} for the Bitter-type solenoid was three times larger than in the case of the electrical measurements in this solenoid because the magnetic field was not measured as a function of solenoid current during each run.
[23]C. Haas, Crit. Rev. Solid State Sci. **1**, 47 (1970).
[24]E. M. Pugh and N. Rostoker, Rev. Mod. Phys. **25**, 151 (1953); S. Foner Phys. Rev. **101**, 1648 (1956).
[25]Y. Shapira and T. B. Reed (unpublished).
[26]C. Kittel, Phys. Rev. Lett. **10**, 339 (1963).
[27]See Ref. 10 and papers quoted here.
[28]P. G. de Gennes and J. Friedel, J. Phys. Chem. Solids **4**, 71 (1958).
[29]D. J. Kim, Prog. Theor. Phys. **31**, 921 (1964).
[30]M. E. Fisher and J. S. Langer, Phys. Rev. Lett. **20**, 665 (1968).
[31]Y. Capiomont, Nguyen-Van-Dang, O. Massenet, and B. K. Chakraverty, Solid State Commun. **10**, 679 (1972).
[32]N. Menyuk, K. Dwight, and T. B. Reed, Phys. Rev. B **3**, 1689 (1971).
[33]D. T. Teaney, in *Critical Phenomena*, edited by S. Green and V. Sengers (U.S. GPO, Washington, D.C., 1965), p. 50.
[34]B. E. Argyle, N. Miyata, and T. D. Schultz, Phys. Rev. **160**, 413 (1967).
[35]M. Rayl and P. J. Wojtowicz, Phys. Lett. A 28, 142 (1968).
[36]P. Leroux-Hugon, Phys. Rev. Lett. **29**, 939 (1972).
[37]H. W. Lehmann, Phys. Rev. **163**, 488 (1967).
[38]F. Rys, J. S. Helman, and W. Baltensperger, Phys. Kondens. Mater. **6**, 105 (1967); W. Baltensperger, J. Appl. Phys. **41**, 1052 (1970).
[39]G. Busch, P. Junod, and P. Wachter, Phys. Lett. **12**, 11 (1964); M. J. Freiser, F. Holtzberg, S. Methfessel, G. D. Pettit, M. W. Shafer, and J. C. Suits, Helv. Phys. Acta **41**, 832 (1968); E. Kaldis, J. Schoenes, and P. Wachter, AIP Conf. Proc. **5**, 269 (1972); P. Wachter, Crit. Rev. Solid State Sci. **3**, 189 (1972).
[40]R. A. Smith, *Semiconductors* (Cambridge U.P., Cambridge, England, 1959), Sec. 4.3.
[41]At 298 K the difference between R and R_0 in our samples was $\sim 1\%$.
[42]T. Kasuya, Prog. Theor. Phys. **16**, 58 (1956).
[43]C. Haas, Phys. Rev. **168**, 531 (1968); and IBM J. Res. Dev. **14**, 282 (1970).